Amyloid

Deutsche Ausgabe: DOI: 10.1002/ange.201507092
Internationale Ausgabe: DOI: 10.1002/anie.201507092

Delineating the Role of Helical Intermediates in Natively Unfolded Polypeptide Amyloid Assembly and Cytotoxicity

*Carole Anne De Carufel, Noé Quittot, Phuong Trang Nguyen, and Steve Bourgault**

Abstract: *Amyloid deposition is a hallmark of many diseases, such as the Alzheimer's disease. Numerous amyloidogenic proteins, including the islet amyloid polypeptide (IAPP) associated with type II diabetes, are natively unfolded and need to undergo conformational rearrangements allowing the formation of locally ordered structure(s) to initiate self-assembly. Recent studies have indicated that the formation of α-helical intermediates accelerates fibrillization, suggesting that these species are on-pathway to amyloid assembly. By identifying an IAPP derivative with a restricted conformational ensemble that co-assembles with IAPP, we observed that helical species were off-pathway in homogenous environment and in presence of lipid bilayers or glycosaminoglycans. Moreover, preventing helical folding potentiated membrane perturbation and IAPP cytotoxicity, indicating that stabilization of helical motif(s) is a promising strategy to prevent cell degeneration associated with amyloidogenesis.*

Protein aggregation and amyloid deposition are associated with several diseases, including Alzheimer's disease and type II diabetes.[1] More than 30 proteins have been identified as precursors of amyloids whose deposition is linked to cellular degeneration.[1] While fibrils assembled from these proteins display common structural characteristics, amyloid precursors share no sequence or native state structure homologies.[1] Amyloidogenic polypeptides can be assigned to two different structural classes; those that are natively unfolded and those that show a well-defined structure in their soluble state. Natively folded proteins need to partially unfold, or misfold, in order to form amyloids. In contrast, intrinsically disordered polypeptides (IDPs), such as the amyloid-β peptide (Aβ) and the islet amyloid polypeptide (IAPP), need to undergo conformational rearrangements allowing the formation of locally ordered structure(s) to self-assemble.[2] Cell and animal models have shown that intermediate species of the amyloidogenic cascade are more deleterious than fibrils.[3] Although the molecular structure(s) of the proteotoxic species and the mechanisms of cytotoxicity are still unknown, these studies reinforce the importance of elucidating the initial conformational rearrangements that trigger amyloidogenesis.

[*] C. A. De Carufel, N. Quittot, P. T. Nguyen, Prof. S. Bourgault
Department of Chemistry, Université du Québec à Montréal, Quebec Network for Research on Protein Function, Structure and Engineering (PROTEO)
C.P. 8888, Montréal (Canada)
E-mail: bourgault.steve@uqam.ca

Supporting information for this article is available on the WWW under http://dx.doi.org/10.1002/anie.201507092.

IAPP is the main component of amyloid deposits observed in the pancreatic islets of type II diabetes patients and the amyloidogenic process is known to exacerbate pancreatic β-cell loss.[4] The current view implies that IAPP cytotoxicity is mediated by oligomers and/or prefibrillar aggregates that can be either on- or off-pathway to amyloid formation.[2,5] This 37-residue hormone exhibits a disordered conformation, although it diverges from an absolute random coil by the presence of local and transient helical structures.[6] In membrane environment, IAPP adopts a α-helix that spans between A5 to N22.[7] Recent findings have suggested that IAPP helical conformation represents key structural motif for the intermolecular recognition that initiates assembly and that α-helical oligomers are relevant to toxic functions.[8] Helical intermediate species could be important for the aggregation and toxicity of amyloidogenic IDPs, including Aβ and α-synuclein,[2,9] although this hypothesis is still the matter of active debates.

Two models have been proposed for the conformational rearrangements that initiate IAPP oligomerization and drive amyloid formation. On the one hand, it was proposed that IAPP early oligomerization steps include the formation of β-strand rich dimers and that amyloids are assembled from ordered β-hairpins.[10] On the other hand, the helical intermediates model proposes that association is thermodynamically linked to helix formation within the 5–22 segment. Helical oligomers would generate a high local concentration of the C-terminal amyloidogenic segment, favoring the formation of intermolecular β-sheets.[2] Detecting transient intermediate species of the amyloidogenic cascade by spectroscopic approaches is challenging, particularly in the context of the interactions with biological factors that are relevant to in vivo deposition. Assessing if these intermediates are either on- or off-pathway to fibril formation is even more demanding. An alternative strategy to probe transitions that initiate IDP self-assembly could consist of introducing discrete chemical modifications to restrict the conformational ensemble. Destabilizing on-pathway species should delay, or inhibit, amyloid formation whereas disrupting off-pathway species should either not affect fibrillization or accelerate it by closing a competing pathway. However, it is crucial that this modification does not lead to an alternative pathway.

In this study, we investigated the role of helical intermediates in amyloid formation and induced-cytotoxicity by restricting the conformational ensemble of IAPP. Analogs in which two adjacent residues of IAPP putative helical region are successively substituted by their corresponding D-enantiomers were designed (Supporting Information). Incorporation of two D-residues within a α-helix is known to result in a local disturbance without modifying significantly the

physicochemical properties.[11] Among all derivatives evaluated, [f[15], l[16]]hIAPP, or D-hIAPP, was unique for its random coil structure that persists in presence of the helical-inducing solvent trifluorethanol (TFE) and for its kinetics of fibrillization. By circular dichroism (CD) spectroscopy, hIAPP and D-hIAPP exhibited spectra with a single minimum at 203 nm, indicative of a random coil structure (Figure 1a). Incorporation of D-residues at positions 15 and 16 prevented TFE-induced helical folding of IAPP (Figure 1).

The effect of this modification on amyloid assembly was evaluated using thioflavin T (ThT) fluorescence, atomic force microscopy (AFM) and transmission electron microscopy (TEM). ThT is a dye that fluoresces upon its binding to protein aggregates rich in cross-β-sheets. Under the conditions of fibrillization, hIAPP displayed a T_{50} of 9.86 ± 1.41 h whereas D-hIAPP exhibited a similar kinetics with a T_{50} of 9.33 ± 0.73 h (Figure 1c). At all concentrations evaluated, D-hIAPP and hIAPP had equivalent kinetics of self-assembly (Figure 1d). By AFM and TEM, D-hIAPP fibrils were significantly longer than the ones from hIAPP while both amyloid preparations had comparable average height (Figure 1e,f; Supporting Information for characterization). Although fibrils formed by D-hIAPP and hIAPP were different at the macroscopic level, CD spectroscopy revealed a comparable secondary structure within these assemblies (Supporting Information). Moreover, both sonicated amyloids were competent to seed fibril growth with an equivalent potency (Supporting Information), suggestive of structural similarities. As revealed by solid state NMR, IAPP fibrils consist of two columns of symmetry related monomers and each monomer contains two β-strands connected by a bend-loop.[12] In this model, residues F15 and L16 are in the β-strand that is located on the outer surface of the column. Inversion of the chirality of these two residues most likely affects side-chain orientations within this strand and can modulate lateral association of protofilaments and/or monomer addition.

The equivalent kinetics of nucleation (T_{50} and lag phase) suggests that both peptides could undergo similar conformational rearrangements to initiate self-assembly. To evaluate this hypothesis, equimolar of hIAPP and its D,D-counterpart were mixed together and the kinetics of fibrillization was measured. Strikingly, the kinetics of amyloid formation of 6.25 μM hIAPP mixed with 6.25 μM D-hIAPP were equivalent to a homogenous 12.5 μM solution of hIAPP or D-hIAPP alone, with a T_{50} of 10.02 ± 0.96 h (Figure 2a). Similar results were obtained for total concentrations from 6.25 to 50 μM. Fibrils obtained from a mixture of hIAPP/D-hIAPP were morphologically equivalent to D-hIAPP assemblies (Figure 2b). Incorporation of D-residues at positions 15 and 16 in the non-amyloidogenic rodent IAPP (rIAPP) led to a sharp decrease of its helical folding whereas no effect on its amyloidogenecity was observed (Supporting Information). Taken together, fibril formation kinetics and co-assembly experiments suggest that helical species are off-pathway to amyloid assembly in an aqueous solution.

Amyloid formation in vivo takes place in a complex environment and amyloids extracted from patients are associated with components of the extracellular matrix (ECM) and the plasma membrane. Studies have shown that sulfated glycosaminoglycans (GAGs) and lipid membranes hasten fibrillogenesis. Upon binding to GAGs or anionic membranes, IAPP adopts a helical conformation before converting into β-sheets structure.[2,6b,7a,13] As amyloid assembly is faster under conditions that facilitate the formation of

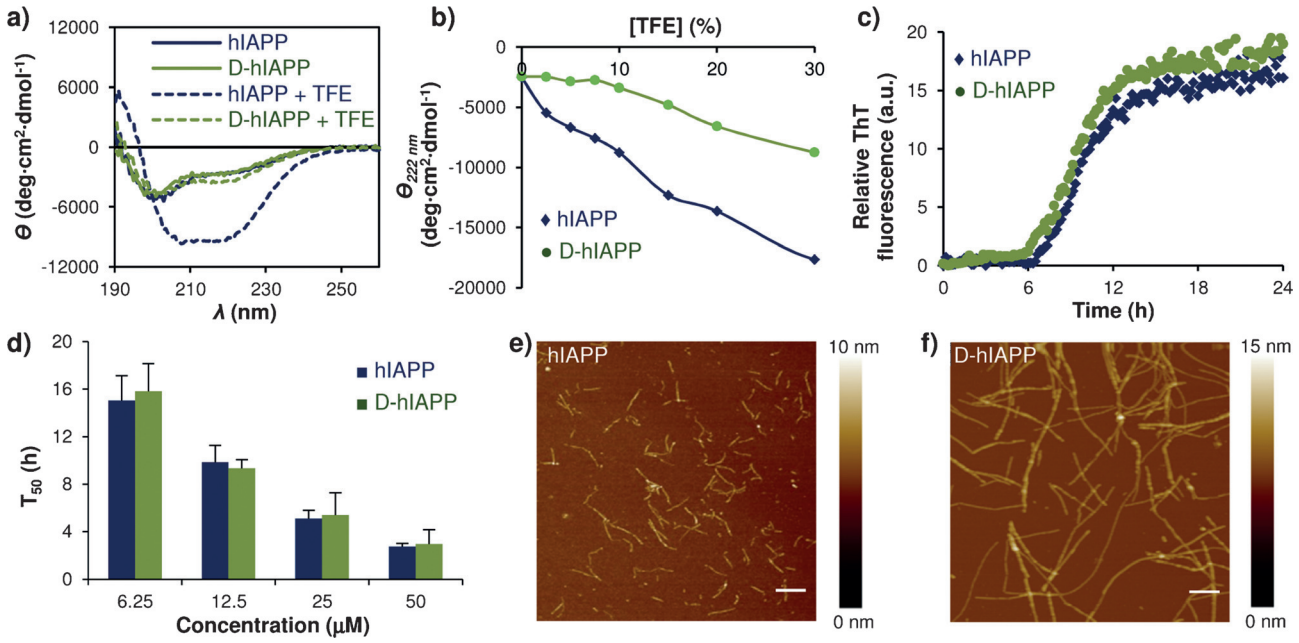

Figure 1. Effect of destabilizing IAPP putative helical domain on amyloid formation. a) CD spectra of 25 μM hIAPP and 25 μM D-hIAPP in Tris-HCl pH 7.4 (solid lines) and in 10% TFE (dashed lines). b) TFE titration into hIAPP and D-hIAPP measured by the ellipticity at 222 nm. c) Amyloid formation monitored by ThT fluorescence of 12.5 μM peptides. d) Rates of amyloid formation at different concentrations. e,f) AFM images of 50 μM hIAPP and D-hIAPP after 24 h incubation. Scale bar: 500 nm.

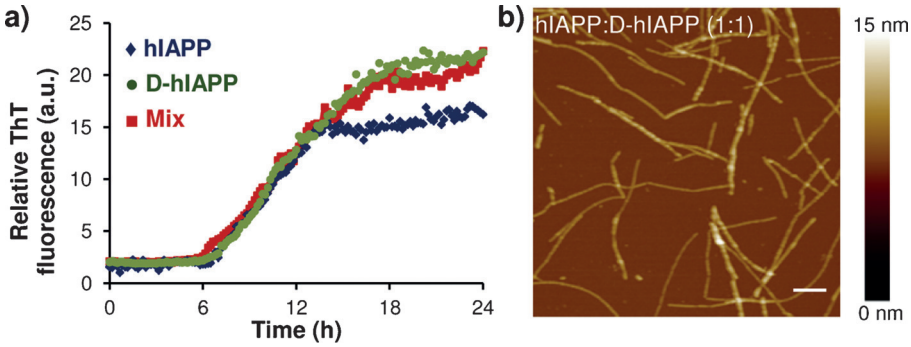

Figure 2. hIAPP and D-hIAPP co-assemble into amyloid fibrils. a) Kinetics of amyloid formation of 12.5 μM hIAPP, D-hIAPP and of a aggregation mixture containing 6.25 μM of hIAPP and 6.25 μM of D-hIAPP (mix). b) AFM images of 25 μM hIAPP mixed with a equimolar concentration of D-hIAPP after 24 h incubation. Scale bar: 500 nm.

nucleating species, these helical intermediates were hypothesized to be on-pathway.[2,8c] Thus, we evaluated the effect of hindering the helical folding of IAPP on the fibrilization kinetics in presence of membrane models and GAGs. When hIAPP was incubated in presence of 100 nm LUVs composed of phosphocholine/phosphoglycerol (DOPC:DOPG 7:3), fibrillization was drastically enhanced (Figure 3a). The accelerating effects of LUVs was more pronounced for D-hIAPP compared to hIAPP, with lag phase of 9.8 ± 4.3 min and 71.2 ± 7.4 min, respectively. Binding of hIAPP to anionic LUVs led to the formation of helical structures (Figure 3b). In contrast, D-hIAPP remained mainly random coil, consistent with the conformational restriction imposed by the D,D-substitution. After 4 h incubation with LUVs, both peptides were converted into β-sheet-rich structure. Conformational conversion, measured with the $\theta_{220}/\theta_{208}$ ratio, correlated closely to the kinetics of amyloid formation measured by ThT-fluorescence (Figure 3c). Similarly, preventing helical folding potentiated the amyloidogenic effect of heparin, employed as a model of the sulfated domains of heparan sulfate (Supporting Information). These data indicate that upon binding to anionic biosurfaces, IAPP undergoes a random coil-to-α-helix conformational conversion and that inhibition of helical formation dramatically hastens self-assembly, suggesting that these species are off-pathway.

Protein deposition in pancreatic islets correlates with β-cell degeneration and several inter-connected mechanisms have been proposed to explain IAPP toxicity.[5] Plasma membrane disruption by pre-fibrillar species, which can trigger various pathways of cell death is one of the most studied mechanisms.[6b] Reports have suggested that the loss of membrane integrity results from pore formation[14] and that helical intermediates could be the active membrane species.[15] In this view, several helical mimetics were recently developed to target the membrane-bound α-helix and to prevent their oligomerization.[8a,16] These compounds were shown to reduce IAPP amyloid formation in presence of membranes and to decrease toxicity. Nonetheless, whether or not these helical species are toxic themselves or are off- or on-pathway to cytotoxicity remains unknown. The helically-frustrated D-hIAPP analog appears as a unique tool to address this question. We initially examined the ability of hIAPP and D-hIAPP to induce leakage of DOPC/DOPG LUVs. The fluorescent dye calcein was encapsulated at high concentration within the vesicles, leading to its self-quenching and upon membrane disruption, the dye is released and fluorescence is restored. Leakage was measured after 10 min and 5 h incubation with lipid/peptide ratios between 6:1 and 80:1.[17] Peptides hIAPP and D-hIAPP induced a similar concentration-dependant vesicle leakage (Figure 4a). The non-amyloidogenic rIAPP and D-rIAPP also induced membrane leakage, although their effects were less pronounced (Supporting Information).

While monitoring the time course of vesicle disruption, a multiphase process was observed for hIAPP; a plateau after 60 min followed by a second phase leading to maximum leakage (Figure 4b and Supporting Information). The second phase correlated closely with formation of ThT-positive species and the kinetics of α-helix-to-β-sheet structural conversion. For the non-amyloidogenic rodent IAPPs, which do not form ThT-positive species in presence of LUVs,

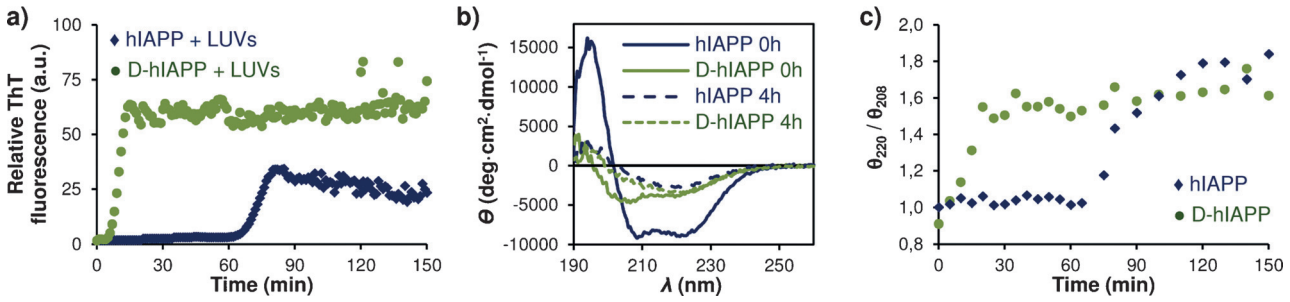

Figure 3. Destabilizing IAPP helical segment potentiates the accelerating effect of model membranes on amyloid formation. a) Kinetics of amyloid formation of 12.5 μM hIAPP and D-hIAPP in presence of 500 μM DOPC/DOPG (7:3) LUVs. b) CD spectra of hIAPP and D-hIAPP in presence of LUVs before (solid lines) and after 4 h incubation (dashed lines). c) Conformational conversion measured by the ratio of ellipticity at 220/208.

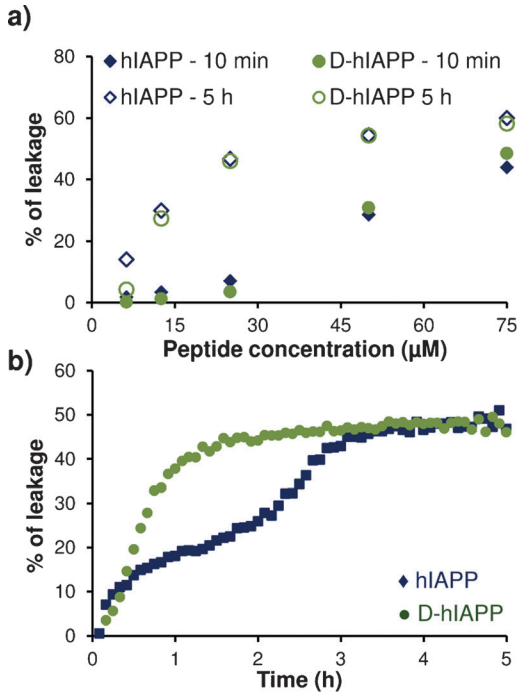

Figure 4. Role of helical intermediates in IAPP-induced membrane leakage. a) Percentage of membrane leakage of DOPC/DOPG (7:3) LUVs by hIAPP and D-hIAPP after 10 min and 5 h incubation (open). b) Kinetics of membrane leakage of DOPC/DOPG (7:3) LUVs by 25 μM hIAPP and D-hIAPP.

a single phase was detected (Supporting Information). This suggests that the first phase of membrane disruption is related to the binding of non-fibrillar species to lipid vesicles and the second phase is mediated by fibril growth.[17,18] This multistep process was not discernable for D-hIAPP, because fibrillization occurs so fast that it cannot be easily discernible from prefibrillar species binding. Vesicle leakage experiments indicated that IAPP helical folding postpones membrane disruption associated with fibril growth.

Next, we evaluated the role of transient helical conformations in toxicity using INS-1 pancreatic β-cells. Treatment with hIAPP induced a concentration-dependent decrease of cellular viability (Figure 5a). Incorporation of a destabilizing motif within hIAPP putative α-helix increased its cytotoxicity. D-hIAPP was not only more cytotoxic but its deleterious effects on viability occurred more rapidly (Figure 5b). After 12 h, hIAPP (50 μM) reduced cellular viability to 63.8 ± 9.0% while a viability of 12.4 ± 2.1% was observed for its D,D-counterpart. To confirm this time-dependent effect and to asses if both peptides used similar mechanisms to induce cell death, caspases activation and intracellular calcium level were measured. A significant increase of apoptosis signal was detected after only 4 h treatment with D-hIAPP whereas a treatment time of 12 h was needed to activate caspases with hIAPP (Figure 5c). Similar effect was observed for cytosolic calcium level, a signal of cellular dysfunction associated with several death mechanisms (Figure 5d). The fact that hindering IAPP helical folding potentiated its toxicity suggests that the formation of α-helix pre-fibrillar species is not required for cell death and it could be even protective.

By identifying a derivative with a restricted conformational ensemble that co-assembles with IAPP, we provided unique insights into the mechanisms of IDP amyloidogenesis. Our results suggest that helical conformations are off-pathway to amyloid formation and delineate the roles of α-helix species in membrane perturbation and toxicity. This study emphasizes that the stabilization of a transient helical motif within an amyloidogenic IDP constitutes a promising strategy to inhibit assembly and to prevent cell degeneration.

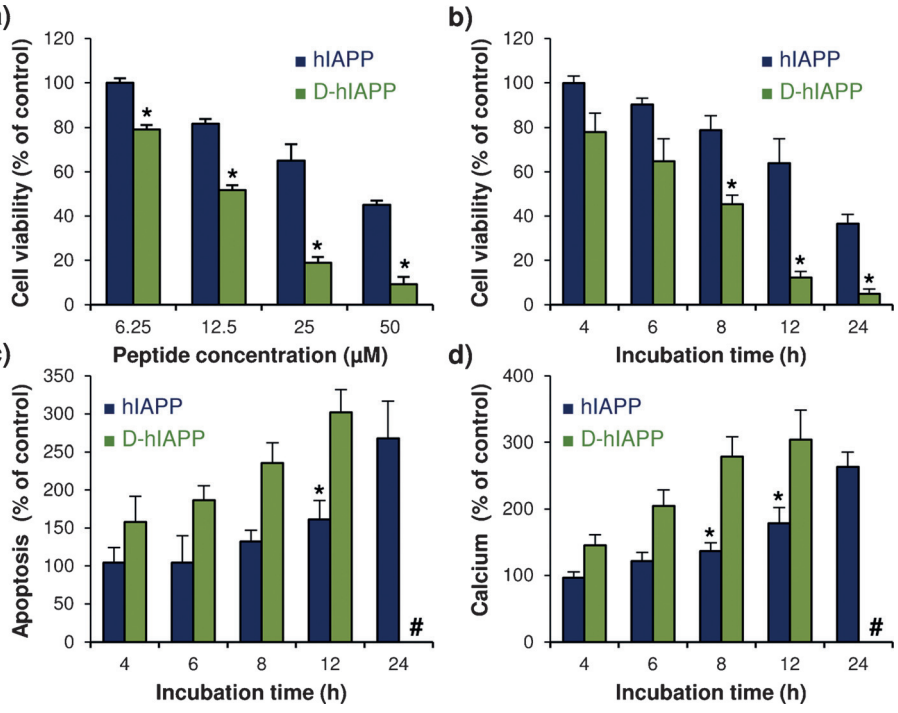

Figure 5. Destabilizing IAPP helical segment potentiates cytotoxicity on pancreatic β-cells. a) Viability of INS-1 cells treated with hIAPP and D-hIAPP for 24 h. b) Kinetics of reduction of INS-1 cell viability by 50 μM of hIAPP and D-hIAPP. c) Caspases 3/7 activation by 50 μM hIAPP and D-hIAPP measured over treatment time. d) Evaluation of intracellular calcium level after treatment with 50 μM hIAPP and D-hIAPP. Results are expressed as percentage of the vehicle treated cells ± S.E.M. * Statistically significant difference between hIAPP and D-hIAPP ($P < 0.05$). # Data could not be obtained because of high extent of cell death.

Acknowledgements

This work was supported by the Natural Sciences and Engineering Research Council of Canada (NSERC; 418614) and the Fonds de recherche du Québec, Nature et technologies (FRQNT)

Keywords: amyloid · glycosaminoglycans · islet amyloid polypeptide · membrane models · α-helix

How to cite: *Angew. Chem. Int. Ed.* **2015**, *54*, 14383 – 14387
Angew. Chem. **2015**, *127*, 14591 – 14595

[1] F. Chiti, C. M. Dobson, *Annu. Rev. Biochem.* **2006**, *75*, 333 – 366.
[2] A. Abedini, D. P. Raleigh, *Protein Eng. Des. Sel.* **2009**, *22*, 453 – 459.
[3] a) R. Kayed, E. Head, J. L. Thompson, T. M. McIntire, S. C. Milton, C. W. Cotman, C. G. Glabe, *Science* **2003**, *300*, 486 – 489; b) A. Demuro, E. Mina, R. Kayed, S. C. Milton, I. Parker, C. G. Glabe, *J. Biol. Chem.* **2005**, *280*, 17294 – 17300; c) S. Bourgault, S. Choi, J. N. Buxbaum, J. W. Kelly, J. L. Price, N. Reixach, *Biochem. Biophys. Res. Commun.* **2011**, *410*, 707 – 713; d) J. J. Meier, R. Kayed, C. Y. Lin, T. Gurlo, L. Haataja, S. Jayasinghe, R. Langen, C. G. Glabe, P. C. Butler, *Am. J. Physiol.* **2006**, *291*, E1317 – 1324.
[4] P. Westermark, A. Andersson, G. T. Westermark, *Physiol. Rev.* **2011**, *91*, 795 – 826.
[5] P. Cao, P. Marek, H. Noor, V. Patsalo, L. H. Tu, H. Wang, A. Abedini, D. P. Raleigh, *FEBS Lett.* **2013**, *587*, 1106 – 1118.
[6] a) J. A. Williamson, A. D. Miranker, *Protein Sci.* **2007**, *16*, 110 – 117; b) J. R. Brender, S. Salamekh, A. Ramamoorthy, *Acc. Chem. Res.* **2012**, *45*, 454 – 462; c) R. Soong, J. R. Brender, P. M. Macdonald, A. Ramamoorthy, *J. Am. Chem. Soc.* **2009**, *131*, 7079 – 7085.
[7] a) R. P. Nanga, J. R. Brender, S. Vivekanandan, A. Ramamoorthy, *Biochim. Biophys. Acta Biomembr.* **2011**, *1808*, 2337 – 2342; b) S. M. Patil, S. Xu, S. R. Sheftic, A. T. Alexandrescu, *J. Biol. Chem.* **2009**, *284*, 11982 – 11991; c) M. Apostolidou, S. A. Jayasinghe, R. Langen, *J. Biol. Chem.* **2008**, *283*, 17205 – 17210; d) J. A. Williamson, J. P. Loria, A. D. Miranker, *J. Mol. Biol.* **2009**, *393*, 383 – 396; e) R. P. Nanga, J. R. Brender, J. Xu, K. Hartman, V. Subramanian, A. Ramamoorthy, *J. Am. Chem. Soc.* **2009**, *131*, 8252 – 8261.
[8] a) I. Saraogi, J. A. Hebda, J. Becerril, L. A. Estroff, A. D. Miranker, A. D. Hamilton, *Angew. Chem. Int. Ed.* **2010**, *49*, 736 – 739; *Angew. Chem.* **2010**, *122*, 748 – 751; b) A. Nath, A. D. Miranker, E. Rhoades, *Angew. Chem. Int. Ed.* **2011**, *50*, 10859 – 10862; *Angew. Chem.* **2011**, *123*, 11051 – 11054; c) J. D. Knight, J. A. Hebda, A. D. Miranker, *Biochemistry* **2006**, *45*, 9496 – 9508.
[9] a) M. D. Kirkitadze, M. M. Condron, D. B. Teplow, *J. Mol. Biol.* **2001**, *312*, 1103 – 1119; b) M. Zhu, J. Li, A. L. Fink, *J. Biol. Chem.* **2003**, *278*, 40186 – 40197.
[10] a) N. F. Dupuis, C. Wu, J. E. Shea, M. T. Bowers, *J. Am. Chem. Soc.* **2009**, *131*, 18283 – 18292; b) N. F. Dupuis, C. Wu, J. E. Shea, M. T. Bowers, *J. Am. Chem. Soc.* **2011**, *133*, 7240 – 7243; c) L. E. Buchanan, E. B. Dunkelberger, H. Q. Tran, P. N. Cheng, C. C. Chiu, P. Cao, D. P. Raleigh, J. J. de Pablo, J. S. Nowick, M. T. Zanni, *Proc. Natl. Acad. Sci. USA* **2013**, *110*, 19285 – 19290.
[11] a) A. T. Neree, P. T. Nguyen, D. Chatenet, A. Fournier, S. Bourgault, *FEBS Lett.* **2014**, *588*, 4590 – 4596; b) T. Wieprecht, M. Dathe, M. Schumann, E. Krause, M. Beyermann, M. Bienert, *Biochemistry* **1996**, *35*, 10844 – 10853.
[12] S. Luca, W. M. Yau, R. Leapman, R. Tycko, *Biochemistry* **2007**, *46*, 13505 – 13522.
[13] C. A. De Carufel, P. T. Nguyen, S. Sahnouni, S. Bourgault, *Biopolymers* **2013**, *100*, 645 – 655.
[14] a) N. B. Last, E. Rhoades, A. D. Miranker, *Proc. Natl. Acad. Sci. USA* **2011**, *108*, 9460 – 9465; b) M. Anguiano, R. J. Nowak, P. T. Lansbury, Jr., *Biochemistry* **2002**, *41*, 11338 – 11343.
[15] M. Magzoub, A. D. Miranker, *FASEB J.* **2012**, *26*, 1228 – 1238.
[16] a) J. A. Hebda, I. Saraogi, M. Magzoub, A. D. Hamilton, A. D. Miranker, *Chem. Biol.* **2009**, *16*, 943 – 950; b) S. Kumar, D. E. Schlamadinger, M. A. Brown, J. M. Dunn, B. Mercado, J. A. Hebda, I. Saraogi, E. Rhoades, A. D. Hamilton, A. D. Miranker, *Chem. Biol.* **2015**, *22*, 369 – 378.
[17] P. Cao, A. Abedini, H. Wang, L. H. Tu, X. Zhang, A. M. Schmidt, D. P. Raleigh, *Proc. Natl. Acad. Sci. USA* **2013**, *110*, 19279 – 19284.
[18] J. R. Brender, E. L. Lee, K. Hartman, P. T. Wong, A. Ramamoorthy, D. G. Steel, A. Gafni, *Biophys. J.* **2011**, *100*, 685 – 692.

Received: July 30, 2015
Revised: September 4, 2015
Published online: October 6, 2015

